Accepted Manuscript

Synthesis and Quantitative Structure–activity Relationships Study for Phenylpropenamide Derivatives as Inhibitors of Hepatitis B Virus Replication

Yang Jing, Ma Min, Wang Xueding, Jiang Xingjun, Zhang Yuanyuan, Yang Weiqing, Li Zicheng, Wang Xihong, Yang bin, Ma Menglin

PII: S0223-5234(15)30059-3

DOI: 10.1016/j.ejmech.2015.05.032

Reference: EJMECH 7911

To appear in: *European Journal of Medicinal Chemistry*

Received Date: 11 November 2014

Revised Date: 29 March 2015

Accepted Date: 21 May 2015

Please cite this article as: Y. Jing, M. Min, W. Xueding, J. Xingjun, Z. Yuanyuan, Y. Weiqing, L. Zicheng, W. Xihong, Yang bin, M. Menglin, Synthesis and Quantitative Structure–activity Relationships Study for Phenylpropenamide Derivatives as Inhibitors of Hepatitis B Virus Replication, *European Journal of Medicinal Chemistry* (2015), doi: 10.1016/j.ejmech.2015.05.032.

Synthesis and Quantitative Structure–activity Relationships Study for Phenylpropenamide Derivatives as Inhibitors of Hepatitis B Virus Replication

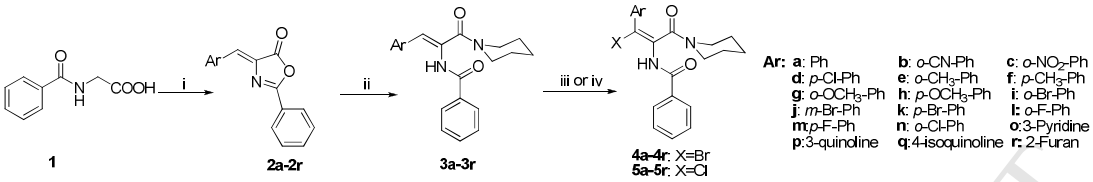

The new phenylpropenamide derivatives were synthesized, characterized and evaluated for their anti-HBV activities. The 2D and 3D-QSAR models of phenylpropenamide was constructed.

Synthesis and Quantitative Structure–activity Relationships Study for Phenylpropenamide Derivatives as Inhibitors of Hepatitis B Virus Replication

Yang Jing[a], Ma Min[a], Wang Xueding[a], Jiang Xingjun[a], Zhang Yuanyuan[a, b]*, Yang Weiqing[a], Li Zicheng[b], Wang Xihong[a], Yang bin[c], Ma Menglin[a]*

[a] Key Lab of Advanced Scientific Computation of Sichuan province, Faculty of physical and chemistry, Xihua University, Chengdu 610039, China

[b] College of chemical engineering, Sichuan University, Chengdu 610065, China

[c] West china school of pharmacy, Sichuan University, Chengdu 610064, China

Abstract A series of new phenylpropenamide derivatives containing different substituents was synthesized, characterized and evaluated for their anti-hepatitis B virus (HBV) activities. The quantitative structure–activity relationships (QSAR) of phenylpropenamide compound have been studied. The 2D-QSAR models, based on DFT and multiple linear regression analysis methods, revealed that higher values of total energy (*TE*) and lower entropy (S^o) enhanced the anti-HBV activities of the phenylpropenamide molecules. Predictive 3D-QSAR models were established using SYBYL multifit molecular alignment rule. The optimum models were all statistically significant with cross-validated and conventional coefficients, indicating that they were reliable enough for activity prediction.

Keywords Phenylpropenamide, DFT, QSAR, Hepatitis B

1. Introduction

The treatment of hepatitis B virus infection represents one of the current therapeutic challenges in virology. There are approximately 350 million chronically infected individuals, resulting in 0.5-1.2 million deaths annually [1-3]. Although interferon-α has been a mainstay of HBV treatment regimens, sustained response rates tend to be low (20±30%) and resistance builds rapidly [4-5]. The other current agents approved for the treatment of HBV infection are nucleoside analogues lamivudine, telbivudine, entecavir, adefovir and tenofovir (Fig. 1) [6-9] .

Phenylpropenamides (Fig. 2), such as AT-61 [10] and AT-130 [11-14], were reported as a non-nucleoside class of inhibitors of HBV replication in cell culture. It was also reported that phenylpropenamides were specific inhibitors of HBV replication and most likely inhibited replication by interfering with the packaging of pregenomic RNA into immature core particles.

Structure–activity relationship analysis widely applied due to their well-established predictive power [15]. Essentially, provides an useful tool in new drugs design by correlating the physico-chemical properties of a series of compounds with their respective biological activities. In order to explore the relationship between structure and antiviral activity, a series of phenylpropenamide derivatives was synthesized and their antiviral activities were then tested. The density functional theory (DFT) and linear regression analysis method were used to construct the 2D-QSAR models [16-17]. Furthermore, three-dimensional quantitative structure-activity relationship (3D-QSAR) method is helpful to extract a relation between biological activity and chemical structure. Especially, the comparative molecular field analysis (CoMFA) is an effective method based on statistical techniques [18-20]. The biological activity of new phenylpropenamide derivatives can be predicted by using the 2D or 3D-QSAR equation, which may offers an important reference for the future research work on novel derivative design and synthesis.

2. Experimental

2.1 Chemistry

Thin layer chromatography was performed with Qingdao Ocean silica gel GF254. Nuclear magnetic resonance (NMR) spectra were recorded on a Bruker DPX-300 FT NMR spectrometer at 300 MHz for ^{1}H and were referenced to tetramethylsilane (δ values are given in ppm and *J*-values in Hz). HRMS were measured on Shimadzu LCMS-IT-TOF. ESI-MS were measured on a Varian CH-5 apparatus. IR spectra were measured acquired on a Nicolet 380 and obtainedby using KBr platespellet. The X-ray diffraction data were collected on X'Pert Pro MPD diffract meter. The synthetic route was shown in Scheme 1.

2.1.1 General procedure for the preparation of 4-arylidene-2-phenyloxazol-5(4H)-one (**2a-2r**)

Hippuric acid (10 g, 56 mmol), aromatic aldehydes (43 mmol), potassium acetate (4.22 g, 44 mmol) and acetic anhydride (14mL, 17 mmol) were added to a 100 mL three-necked flask and heated at reflux for 0.5 h. The reaction mixture was treated with ethanol (20 mL) when the temperature was cooled down to 40 ^{o}C. The product was further found by precipitation as the temperature went down to ambient. The resulting solid was collected, washed with ethanol (2×10 mL) and then dried to obtain **2a-2r** as yellow crystals.

2.1.2 General procedure for the preparation of *N*-(3-oxo-1-aryl-3-(piperidin-1-yl)prop-1-en -2-yl)benzamide (**3a-3r**)

Dichloromethane (50 mL) and piperidine (2.83g, 33mmol) were added into a solution of **2** (33mmol) in dichloromethane (166mL) at 0°C, and then stirred at this temperature for 1 h to obtain CH_2Cl_2 solution of **3a-3r**, which were used for the next reaction without further purification.

2.1.3 General procedure for the preparation of (*Z*)-*N*-(1-bromo-3-oxo-1-aryl-3-(piperidin-1-yl) prop-1-en-2-yl) benzamide (**4a-4r**)

Solid calcium carbonate (4.16 g, 42 mmol) was added to a dichloromethane solution of **3a-3r** at 0 ^{o}C, and bromine liquid (5.32 g, 33mmol) in CH_2Cl_2 (50mL) was then added to the mixture. The resulting solution was stirred at room temperature overnight, filtered and evaporated to afford the yellow oil, which was finally crystallized from ethanol to give **4a-4r**

2.1.4.1 (*Z*)-*N*-(1-chloro-3-oxo-1-phenyl-3-(piperidin-1-yl)prop-1-en-2-yl)benzamide (**5a**). White crystals. Yield 16%; ^{1}H NMR (300MHz, $CDCl_3$): 8.14 (s, 1H, NH), 7.92 (d, *J*=7.2Hz, 2H, ArH), 7.61 (m, 5H, ArH), 7.39 (t, *J*=3Hz, 3H, ArH), 3.65 (m, 1H, CH_2), 3.33 (m, 3H, CH_2), 1.56 (m, 4H, CH_2), 1.12 (m, 1H, CH_2), 0.53 (m, 1H, CH_2), IR (KBr, cm^{-1}) *v*: 3446 (NH), 2360 (C-H), 1650, 1544 (C=O), 1268 (C=C), 1089, 790. ESI-MS 2m/z: 736.72.

2.1.4.2 (*Z*)-*N*-(1-chloro-1-(2-cyanophenyl)-3-oxo-3-(piperidin-1-yl)prop-1-en-2-yl)benzamide (**5b**). Pale yellow crystals. Yield 11%; ^{1}H NMR (300MHz, $CDCl_3$): 8.27 (s, 1H, NH), 7.92 (d, *J*=7.8Hz, 2H, ArH), 7.79 (d, *J*=7.5Hz, 1H, ArH), 7.68 (m, 3H, ArH), 7.54 (t, *J*=7.5Hz, 3H, ArH), 3.37 (s, 4H, CH_2), 1.91 (m, 1H, CH_2), 1.45 (m, 3H, CH_2), 1.01 (m, *J*=3.6Hz, 2H, CH_2), IR (KBr, cm^{-1}) *v*: 3293 (NH), 2882 (C-H), 2225 (CN), 1662, 1618 (C=O), 1268 (C=C), 1025, 709.

^{13}C NMR (75Hz, $CDCl_3$): δ 164.34, 161.89, 135.67, 133.36, 132.87. 132.61, 132.53, 132.14, 130.83, 128.75, 128.42, 127.67, 124.60, 115.88, 106.34, 47.86, 42.63, 25.61, 24.82, 24.14. HRMS (EI) calcd. for 393.1244; $C_{22}H_{20}ClN_3O_2$, found (E^+) 394.1323.

2.1.4.3 (*Z*)-*N*-(1-chloro-1-(2-nitrophenyl)-3-oxo-3-(piperidin-1-yl)prop-1-en-2-yl)benzamide (**5c**). Pale yellow crystals. Yield 28%; ^{1}H NMR (300MHz, $CDCl_3$): 8.23 (s, 1H, NH), 8.09 (d, *J*=7.5Hz, 1H, ArH), 7.93 (d, *J*=7.2Hz, 2H, ArH), 7.63 (d, *J*=6.6Hz, 1H, ArH), 7.67 (m, 5H, ArH), 3.46 (m,

4H, CH_2), 1.78 (m, *J*=0.3Hz, 1H, CH_2), 1.43 (m, 5H, CH_2), IR (KBr, cm^{-1}) *v*: 3273 (NH), 2932 (C-H), 1652, 1618 (C=O), 1268 (C=C), 910, 740. ^{13}C NMR (75Hz, $CDCl_3$): δ 164.15, 162.19, 136.22, 135.44, 133.35, 132.84. 132.51, 132.63, 132.37, 130.87, 128.91, 127.45, 124.64, 106.80, 47.93, 42.67, 25.42, 24.85, 24.17. HRMS (EI) calcd. for 413.1142; $C_{21}H_{20}ClN_3O_4$, found (E^+) 414.1221.

2.1.4.4 (*Z*)-*N*-(1-chloro-1-(4-chlorophenyl)-3-oxo-3-(piperidin-1-yl)prop-1-en-2-yl)benzamide (**5d**). White crystals. Yield 3%; ^1H NMR (300MHz, $CDCl_3$): 8.11 (s, 1H, NH), 7.91 (d, *J*=7.2Hz, 2H, ArH), 7.62 (t, *J*=7.2Hz, 1H, ArH), 7.53 (t, *J*=8.4Hz, 4H, ArH), 7.37 (d, *J*=8.4Hz, 2H, ArH), 3.52 (m, 3H, CH_2), 3.12 (m, 1H, CH_2), 1.64 (s, 4H, CH_2), 1.48 (m, 2H, CH_2), IR (KBr, cm^{-1}) *v*: 3270 (NH), 2858 (C-H), 1672, 1623 (C=O), 1267 (C=C), 1092, 707. ESI-MS 2m/z: 805.66.

2.1.4.5 (*Z*)-*N*-(1-chloro-3-oxo-3-(piperidin-1-yl)-1-o-tolylprop-1-en-2-yl)benzamide (**5e**). White crystals. Yield 11%; ^1H NMR (300MHz, $CDCl_3$): 8.12 (s, 1H, NH), 7.92 (d, *J*=7.2Hz, 2H, ArH), 7.61 (m, 3H, ArH), 7.37 (s, 2H, ArH), 7.29 (m, 2H, ArH), 3.65 (m, 1H, CH_2), 3.34 (m, 3H, CH_2), 2.38 (s, 3H, CH_3), 1.41 (m, 4H, CH_2), 1.13 (m, 1H, CH_2), 0.53 (m, 1H, CH_2), IR (KBr, cm^{-1}) *v*: 3234 (NH), 2921 (C-H), 1662, 1616 (C=O), 1289 (C=C), 1034, 790. ESI-MS MS 2m/z: 764.81.

2.1.4.6 (*Z*)-*N*-(1-chloro-3-oxo-3-(piperidin-1-yl)-1-p-tolylprop-1-en-2-yl)benzamide (**5f**). White crystals. Yield 16%; ^1H NMR (300MHz, $CDCl_3$): 8.11 (s, 1H, NH), 7.92 (d, *J*=7.5Hz, 2H, ArH), 7.60 (t, *J*=6.9 Hz, 1H, ArH), 7.52 (dd, *J*=7.5Hz, *J*=8.1 Hz, 4H, ArH), 7.19 (d, *J*=8.1Hz, 2H, ArH), 3.55 (m, 3H, CH_2), 3.13 (m, 1H, CH_2), 2.39 (s, 3H, CH_3), 1.58 (m, 4H, CH_2), 1.18 (m, 1H, CH_2), 0.62 (m, 1H, CH_2), IR (KBr, cm^{-1}) *v*: 3282 (NH), 2960 (C-H), 1662, 1635 (C=O), 1268 (C=C), 1025, 810. ESI-MS 2m/z: 764.73.

2.1.4.7 (*Z*)-*N*-(1-chloro-1-(2-methoxyphenyl)-3-oxo-3-(piperidin-1-yl)prop-1-en-2-yl)benzamide (**5g**). White crystals. Yield 11%; ^1H NMR (300MHz, $CDCl_3$): 8.21 (s, 1H, NH), 7.92 (d, *J*=6.9Hz, 2H, ArH), 7.60 (t, *J*=7.2Hz, 1H, ArH), 7.52 (t, *J*=7.8Hz, 2H, ArH), 7.42 (t, *J*=7.5Hz, 2H, ArH), 6.97 (t, *J*＝6.9Hz, 2H, ArH), 3.89 (s, 3H, CH_3), 3.33 (m, 4H, CH_2), 1.53 (m, 4H, CH_2), 0.97 m, 1H, CH_2), 0.78 (m, 1H, CH_2), IR (KBr, cm^{-1}) *v*: 3446 (NH), 2360 (-CH_3), 1652, 1558 (C=O), 1268(C=C), 1093, 790. ESI-MS 2m/z: 796.72.

2.1.4.8 (*Z*)-*N*-(1-chloro-1-(4-methoxyphenyl)-3-oxo-3-(piperidin-1-yl)prop-1-en-2-yl)benzamide (**5h**). White crystals. Yield 13%; ^1H NMR (300MHz, $CDCl_3$): 8.08 (s, 1H, NH), 7.92 (d, *J*=7.2Hz, 2H, ArH), 7.61 (m, 5H, ArH), 6.91 (d, *J*=8.7Hz, 2H, ArH), 3.85 (s, 3H, CH_3), 3.61 (m, 1H, CH_2), 3.40 (m, 2H, CH_2), 3.16 (m, 1H, CH_2), 1.61 (m, 4H, CH_2), 1.20 (m, 1H, CH_2), 0.68 (m, 1H, CH_2), IR (KBr, cm^{-1}) *v*: 3446 (NH), 2360 (-CH_3), 1650, 1553 (C=O), 1268 (C=C), 1089, 790. ESI-MS 2m/z: 796.79.

2.1.4.9 (*Z*)-*N*-(1-(2-bromophenyl)-1-chloro-3-oxo-3-(piperidin-1-yl)prop-1-en-2-yl)benzamide (**5i**). White crystals. Yield 9%; ^1H NMR (300MHz, $CDCl_3$): 8.25 (s, 1H, NH), 7.93 (d, *J*=7.2Hz, 2H, ArH), 7.67 (m, 5H, ArH), 7.36 (m, 2H, ArH), 3.55 (m, 2H, CH_2), 3.36 (m, 1H, CH_2), 3.21 (m, 1H, CH_2), 1.80 (s, 1H, CH_2), 1.59 (m, 4H, CH_2), 0.97 (m, 1H, CH_2), IR (KBr, cm^{-1}) *v*: 3446 (NH), 2360 (-CH_3), 1652, 1558 (C=O), 1268 (C=C), 1091, 799. ^{13}C NMR (75Hz, $CDCl_3$): δ 164.13, 162.14, 135.10, 133.35, 132.65, 132.62, 132.54, 131.09, 131.03, 128.86, 127.50, 127.47, 124.12, 115.84, 47.97, 42.59, 25.35, 24.86, 24.20. HRMS (EI) calcd. for 446.0397; $C_{21}H_{20}BrClN_2O_2$, found (E^+) 449.0481.

2.1.4.10 (*Z*)-*N*-(1-(3-bromophenyl)-1-chloro-3-oxo-3-(piperidin-1-yl)prop-1-en-2-yl)benzamide (**5j**). White crystals. Yield 15%; ^1H NMR (300MHz, $CDCl_3$): 8.19 (s, 1H, NH), 7.91 (d, *J*=8.1Hz, 2H, ArH), 7.71 (s, 1H, ArH), 7.61 (t, *J*=7.8Hz, 1H, ArH), 7.52 (dd, *J*=6.9Hz, *J*=1.2 Hz, 4H, ArH),

7.24 (d, *J*=7.8Hz, 1H, ArH), 3.63 (m, 1H, CH_2), 3.33 (m, 3H, CH_2), 1.61 (m, 4H, CH_2), 1.18 (m, 1H, CH_2), 0.60 (m, 1H, CH_2), IR (KBr, cm^{-1}) *v*: 3243 (NH), 2921 (C-H), 1670, 1618 (C=O), 1268 (C=C), 916, 682. ^{13}C NMR (75Hz, $CDCl_3$): *δ* 164.16, 162.21, 134.78, 133.23, 132.66, 132.59, 132.47, 131.21, 131.01, 128.83, 127.74, 127.43, 124.02, 115.87, 47.86, 42.53, 25.38, 24.82, 24.24. HRMS (EI) calcd. for 446.0397; $C_{21}H_{20}BrClN_2O_2$, found (E^+) 449.0476.

2.1.4.11 (*Z*)-*N*-(1-(4-bromophenyl)-1-chloro-3-oxo-3-(piperidin-1-yl)prop-1-en-2-yl)benzamide (**5k**). White crystals. Yield 6%; ^1H NMR (300MHz, $CDCl_3$): 8.13 (s, 1H, NH), 7.91 (d, *J*=7.5Hz, 2H, ArH), 7.62 (t, *J*=7.2Hz, 1H, ArH), 7.53 (m, 6H, ArH), 3.51 (m, 3H, CH_2), 3.12 (m, 1H, CH_2), 1.61 (m, 4H, CH_2), 1.20 (m, 1H, CH_2), 0.71 (m, 1H, CH_2), IR (KBr, cm^{-1}) *v*: 3322 (NH), 2903 (C-H), 1691, 1618 (C=O), 1268 (C=C), 1016 (C-H), 593 (Ar-H). ^{13}C NMR (75Hz, $CDCl_3$): *δ* 164.21, 162.28, 133.96, 132,62, 132.61, 131.48, 130.32, 129.08, 128.87, 127.47, 123.55, 116.87, 47.79, 42.51, 24.84, 24.52, 24.15. HRMS (EI) calcd. for 446.0397; $C_{21}H_{20}BrClN_2O_2$, found (E^+) 449.0471 .

2.1.4.12 (*Z*)-*N*-(1-chloro-1-(2-fluorophenyl)-3-oxo-3-(piperidin-1-yl)prop-1-en-2-yl)benzamide (**5l**). White crystals. Yield 21%; ^1H NMR (300MHz, $CDCl_3$): 8.22 (s, 1H, NH), 7.93 (d, *J*=7.8Hz, 2H, ArH), 7.62 (m, 5H, ArH), 7.18 (dd, *J*=6.6Hz, *J*=8.7Hz, 2H, ArH), 3.46 (m, 4H, CH_2), 1.57 (m, 4H, CH_2), 1.01 (m, 2H, CH_2), IR (KBr, cm^{-1}) *v*: 3234 (NH), 2853 (C-H), 1652, 1618 (C=O), 1268 (C=C), 1025, 761. ESI-MS 2m/z: 772.95.

2.1.4.13 (*Z*)-*N*-(1-chloro-1-(4-fluorophenyl)-3-oxo-3-(piperidin-1-yl)prop-1-en-2-yl)benzamide (**5m**). White crystals. Yield 4%; ^1H NMR (300MHz, $CDCl_3$): 8.11 (s, 1H, NH), 7.91 (d, *J*=7.5Hz, 2H, ArH), 7.62 (s, 5H, ArH), 7.11 (t, *J*=8.7Hz, 2H, ArH), 3.58 (m, 1H, CH_2), 3.39 (m, 2H, CH_2), 3.16 (m, 1H, CH_2), 1.62 (m, 4H, CH_2), 1.17 (m, 1H, CH_2), 0.65 (m, 1H, CH_2), IR (KBr, cm^{-1}) *v*: 3273 (NH), 2862 (C-H), 1691, 1618 (C=O), 1268 (C=C), 1025, 746. ESI-MS MS 2m/z: 772.95.

2.1.4.14 (*Z*)-*N*-(1-chloro-1-(2-chlorophenyl)-3-oxo-3-(piperidin-1-yl)prop-1-en-2-yl)benzamide (**5n**). White crystals. Yield 24%; ^1H NMR (300MHz, $CDCl_3$): 8.25 (s, 1H, NH), 7.93 (d, *J*=7.2Hz, 2H, ArH), 7.62 (t, *J*=7.2Hz, 1H, ArH), 7.53 (dd, *J*=7.8Hz, *J*=9Hz, 4H, ArH), 7.39 (m, 2H, CH_2), 3.50 (m, 4H, CH_2), 1.58 (m, 4H, CH_2), 0.97 (m, 2H, CH_2), IR (KBr, cm^{-1}) *v*: 3270 (NH), 2931 (C-H), 1662, 1618 (C=O), 1268 (C=C), 1025, 742. ^{13}C NMR (75Hz, $CDCl_3$): *δ* 164.22, 162.15, 135.46, 134.47, 132.67, 132.58, 132.43, 131.27, 131.12, 128.98, 127.53, 127.45, 124.10, 115.89, 47.86, 42.52, 25.44, 24.85, 24.18. HRMS (EI) calcd. for 402.0902; $C_{21}H_{20}Cl_2N_2O_2$, found (E^+) 403.0981.

2.1.4.15 (*Z*)-*N*-(1-chloro-3-oxo-3-(piperidin-1-yl)-1-(yridine-3-yl)prop-1-en-2-yl)benzamide (**5o**) White crystals. Yield 6%; ^1H NMR (300MHz, $CDCl_3$): 8.80 (s, 1H, NH), 8.60 (s, 1H, ArH), 8.21 (s, 1H, ArH), 7.91 (d, *J*=7.2Hz, 3H, ArH), 7.63 (t, *J*=10.2Hz, 1H, ArH), 7.53 (t, *J*=7.5Hz , 2H, ArH), 7.35 (t, *J*=5.7Hz, 1H, ArH), 3.54 (m, 2H, CH_2), 3.19 (m, 2H, CH_2), 1.71 (m, 5H, CH_2), 0.66 (m, 1H, CH_2), IR (KBr, cm^{-1}) *v*: 3648 (NH), 2931 (C-H), 1662, 1618 (C=O), 1268 (C=C), 1025, 709. ^{13}C NMR (75Hz, $CDCl_3$): *δ* 164.23, 162.24, 135.43, 132.69, 132.55, 132.40, 131.22, 131.01, 128.97, 127.52, 127.43, 124.32, 115.82, 47.83, 42.54, 25.31, 24.76, 24.25. HRMS (EI) calcd. for 369.1244; $C_{21}H_{20}Cl_2N_2O_2$, found (E^+) 370.1323.

2.1.4.16 (*Z*)-*N*-(1-chloro-3-oxo-3-(piperidin-1-yl)-1-(quinolin-3-yl)prop-1-en-2-yl)benzamide(**5p**) Pale green crystals. Yield 22%; ^1H NMR (300MHz, $CDCl_3$): 9.13 (s, 1H, NH), 8.34 (s, 1H, ArH), 8.23 (s, 1H, ArH), 8.25 (d, *J*=6Hz, 1H, ArH), 7.97 (d, *J*=6Hz, 2H, ArH),7.84 (d, *J*=6Hz, 1H, ArH), 7.54 (t, *J*=6Hz, 1H, ArH), 7.35 (m, 2H, ArH), 7.21 (t, *J*=6Hz, 2H, ArH), 3.79 (m, 2H, CH_2), 3.40 (m, 2H, CH_2), 1.42 (m, 4H, CH_2), 0.11 (m, 2H, CH_2). IR (KBr, cm^{-1}) *v*: 3236 (NH), 2939 (C-H),

1670, 1628 (C=O), 1270 (C=C), 1030, 747. ^{13}C NMR (75Hz, $CDCl_3$): δ 164.15, 161.83, 150.32, 136.23, 134.78, 132.86, 132.73, 130.72, 130.63, 129.45, 129.12, 128.93, 128.18, 127.55, 127.34, 126.86, 100.98, 47.65, 42.42, 24.83, 24.52, 23.93. HRMS (EI) calcd. for 419.1401; $C_{24}H_{22}ClN_3O_2$, found (E^+) 420.1480.

2.1.4.17 (*Z*)-N-(1-chloro-1-(isoquinolin-4-yl)-3-oxo-3-(piperidin-1-yl)prop-1-en-2-yl) benzamide (**5q**) Pale green crystals. Yield 21%; ^{1}H NMR (300MHz, CDCl3): 9.05 (s, 1H, NH), 8.33 (s, 1H, ArH), 8.27 (s, 1H, ArH), 8.25 (d, *J*=6Hz, 1H, ArH), 7.93 (d, *J*=6Hz, 2H, ArH),7.89 (d, *J*=6Hz, 1H, ArH), 7.80 (t, *J*=6Hz, 1H, ArH), 7.62 (m, 2H, ArH), 7.51 (t, *J*=6Hz, 2H, ArH), 3.88 (m, 2H, CH_2), 3.33 (m, 2H, CH_2), 1.32 (m, 4H, CH_2), 0.29 (m, 2H, CH_2). IR (KBr, cm^{-1}) *v*: 3250 (NH), 2946 (C-H), 1671, 1628 (C=O), 1266 (C=C), 1038 (C-H), 742 (Ar-H). ^{13}C NMR (75Hz, $CDCl_3$): δ 164.37, 161.77, 151.56, 136.34, 132.88, 132.63, 130.31, 129.29, 129.12, 129.03, 128.93, 128.42, 127.62, 127.57, 126.89, 125.94, 99.97, 47.83, 42.35, 24.84, 24.47, 23.89. HRMS (EI) calcd. for 419.1401; $C_{24}H_{22}ClN_3O_2$, found (E^+) 420.1480.

2.1.4.17 (Z)-N-(1-chloro-1-(furan-2-yl)-3-oxo-3-(piperidin-1-yl)prop-1-en-2-yl)benzamide (**5r**) White crystals. Yield 4%; ^{1}H NMR (300MHz, $CDCl_3$): 9.19 (s, 1H, NH), 7.96 (d, *J*=10.2Hz, 2H, ArH), 7.59 (m, 4H, ArH), 6.34 (s, 1H, ArH), 5.75 (s, 1H, ArH), 3.71 (d, *J*=2.4Hz, 4H, CH_2), 1.71 (s, 6H, CH_2), IR (KBr, cm^{-1}) *v*: 3322 (NH), 2931 (C-H), 1662, 1618 (C=O), 1268 (C=C), 1025 (C-H), 724 (Ar-H). ^{13}C NMR (75Hz, $CDCl_3$): δ 164.25, 162.10, 135.33, 133.24, 132.89, 132.43, 132.23, 131.11, 128.83, 127.57, 124.02, 116.86, 47.89, 42.53, 25.32, 24.85, 24.19. HRMS (EI) calcd. for 358.1084; $C_{19}H_{19}ClN_2O_2$, found (E^+) 359.1163.

2.2 Crystal data for compound **4j**

The crystal data of the rearranged product were shown as follows. Crystal Data for $C_{21}H_{20}Br_2N_2O_2$ (*M* =492.21): monoclinic, space group $P2_1/c$ (no. 14), a = 9.9091(7) Å, b = 11.9717(5) Å, c = 17.1808(10) Å, β = 106.799(7)°, V = 1951.2(2) Å^3, Z = 4, T = 293.15 K, μ(MoKα) = 4.174 mm^{-1}, *Dcalc* = 1.676 g/mm^3, 11717 reflections measured ($6.01 \leq 2\Theta \leq 52.744$), 3966 unique ($R_{int}$ = 0.0342, R_{sigma} = 0.0468) which were used in all calculations. The final R_1 was 0.0439 ($I > 2\sigma(I)$) and wR_2 was 0.0967. The full crystallographic details of the rearranged product have been deposited at the Cambridge Crystallographic Data Center were allocated the deposition number CCDC 992084 .The crystal structure was shown in Fig 3.

2.3. Biological assay

Anti-HBV activity was evaluated in HepAD38 cellular assay according to literature [21]. It has been found that this series has been found to be generally nontoxic in the HepAD38 cell line even at the highest concentrations tested [4]. The compound **5a** was studied in an additional cell line (HepG2) and found to be similarly nontoxic [22]. This analogue also showed antiviral activity that is specific for HBV. Theresa May Chin Tan commented that this series was able to inhibit the expression of the viral antigens, HBsAg and HBeAg in a concentration-dependent manner with no cytotoxic effects and without any effects on the expression of viral transcripts [23]. So the EC_{50} of compounds were tested and used in QSAR study only. The DNA replication of HBV in the cell was detected by dot blot hybridization and the results were listed in Table 1. The EC_{50} is the concentration of the compound (in μM) which inhibits the synthesis of viral DNA at 50%.

2.4 Computational calculations for 2D-QSAR

All computations were carried out on the Gaussian 09 [24] computer software package. The electronic descriptors were obtained from a single-point calculation at the B3LYP/6-311+g (d) level.

2.4.1 The optimized molecular geometry of compound

The optimized molecular geometry of compound was computed first and the optimized geometrical parameters, such as bond length and total charge of aromatic ring (∑Q of Ar), benzene ring (∑Q of Ph) and a piperidine ring (∑Q of Cy) were given in Table 2.

2.4.2 The parameters for constructing the 2D-QSAR models

Structural parameters include: energy of highest occupied molecular orbital (E_{HOMO}), energy of lowest unoccupied molecular orbital (E_{LUMO}), energy difference between LUMO and HOMO (E_{gap}), the most positive H atom charge (qH^+), molecular averaged polarizability (α) and heat of formation (Δhf) for the structure at 298.15 K and 1 atm (HF). Thermodynamic parameters include: total energy (TE), zero point energy (ZPE), enthalpy (H^{θ}), free energy (G^{θ}), correction value of thermal energy (E_{th}), molar heat capacity at constant volume (CV^{θ}) and entropy (S^{θ}). Some of the quantum chemical parameters were listed in Table 3 and Table 4.

2.5 Molecular modeling and alignment of 3D-QSAR

The 3D-QSAR studies of the phenylpropenamide compounds using the CoMFA performed on the Sybyl 8.0 package running on the Linux operating system. Partial atomic charges of all compounds were calculated by the Gasteigere-Marsili method, and then were optimized for their geometry using Tripos field [25] with a distance-dependent dielectric function and energy convergence criterion of 0.21 kcal/mol Å using the maximum iterations set to 1000 [26].

2.5.1 CoMFA analysis

The improvement of QSAR may originate from the choice of DFT-optimized template and the usage of RMSD-based molecular alignment strategy. To derive the CoMFA descriptor fields, the aligned training set molecules were placed in a 3D cubic lattice with grid spacing of 2Å in x, y, and z directions such that the entire set could be included in it. The CoMFA steric and electrostatic field energies were calculated using a sp3 carbon probe atom with a van derWaals radius of 1.52 Å and a charge of +1.0. Cut-off values for both steric and electrostatic fields were set to 30.0 kcal/mol.

2.5.2 Regression analysis by PLS method

The partial least squares (PLS) methodology analysis with the leave-one-out (LOO) cross-validation procedure was carried out to determine the optimal number of components using the SAMPLS [27]. The cross-validated coefficient q^2, as an internal statistical index of predictive power, was subsequently obtained. The quality of the external prediction was documented using the standard deviation of error prediction (R^2).

3. Results and Discussion

3.1 SAR investigation

SAR investigation of different substitution benzene of phenylpropenamide was done firstly. Compound **4a** showed good activities with EC_{50} of 1.3μM. When the phenylpropenamides have same substituent but different substitution position, the *ortho*-substitution on the aromatic ring provided better anti-HBV activities than *Para*-substitution, such as compounds *o*-Me **4e** and *p*-Me **4f** with EC_{50} of 0.9 and 2.8 μM, the *o*-OMe **4g** and *p*-OMe **4h** with EC_{50} of 2.1 and 8.0 μM respectively. The same anti-HBV activities results exhibited in the vinyl chlorides series **5a-5r** . Michael J. Sofia [4] reported that the *ortho*-substitution on the aromatic can improve anti-HBV activities while *Para*-substitution decreased the antiviral activities. In general, vinyl bromides were slightly more active than corresponding vinyl chlorides.

The compound **4o** and **5o,** where phenyl was replaced by pyridine, have good biological activities with EC_{50} of 1.0 and 0.9 μM respectively. The compound **4r** and **5r** containing furyl subtitude also showed good results. But the compound **4p**, **4q** and **5p**, **5q,** which phenyl group was replaced by quinoline and isoquinoline, have poor biological activity.

3.2 2D-QSAR

The QSAR is fast emerging as an useful tool in modern chemistry, biology, and drug discovery. A 2D-QSAR model is a mathematical equation that correlates the biological, chemical, or physical activity of a molecular system to its geometric and chemical characteristics. The quantum chemical descriptors computed by density functional theory (DFT) have found increasing use in modern QSAR analysis, so the DFT and multiple linear regression analysis method were used to construct the 2D-QSAR models of the phenylpropenamides based on the experimental data of $-\lg(1/EC_{50})$ and the parameters of computational calculations.

To obtain the optimum parameter set for establishing the QSAR model and to remove insignificant descriptors, a preliminary screening of the 21 candidate descriptors were conducted before multiple linear regressions. Table 5 contained the regression equations, and the correlations between every individual descriptor and $-\mathrm{Log}(1/EC_{50})$. All the equations containing a single independent variable were evaluated by regression coefficient *R* and homogeneity of variances *P*. The results in Table 5 showed that *TE* had the highest value of regression coefficient (*R* 0.871) with $-\mathrm{Log}(1/EC_{50})$, which identified that *TE* was the most relevant parameter to the bioactivity indices.

The frontier orbital theory states that the energy of the HOMO and LUMO are the important factors that determine the reactivity of a molecule [28, 29], the $E_{HOMO,}$ E_{LUMO} and ΔE_{gap} was calculated and analyzed firstly. But the single variable equations using E_{HOME}, E_{LUMO} and ΔE_{gap} as parameter appeared nonlinear relationship with the $R < 0.5$ and $P > 0.1$. The result show that there is no any association between the anti-HBV activities of phenylpropenamides and their energy of the HOMO and LUMO.

It was found that the EC_{50} of phenylpropenamide compounds had a certain relation with theoretical data of the thermodynamic parameters, the anti-HBV activities showed a downward trend with the increasing of energy values. The results in Table 5 showed that total energy (*TE*), zero point energy (ZPE), enthalpy (H^{o}) and free energy (G^{o}) have the highest value of regression coefficient with $-\log(1/EC_{50})$, which identified that the these parameters are the most relevant parameter to the bioactivity. The single variable equations using entropy (S^{o}) as parameter has 0.53175 and 0.61512 *R* and 0.02313 and 0.00659 *P* for **4** and **5** series respectively, implying an association between the anti-HBV activities of phenylpropenamide and their S^{o}. The current study presents a comprehensive QSAR analysis for phenylpropenamide as a inhibitors of hepatitis B virus replication drug used energy parameters of total energy (*TE*) and entropy (S^{o}). A multiple regression analysis was carried out and arrived at the final QSAR equation, which can be written as Scheme 2:

where *n* is the number of data points, R^2 is square of the correlation coefficient and represents the goodness of fitting, *F* is the overall *F*-statistics for the addition of each successive term, and *P* is the *P* values using the *F* statistics. Because total energy (*TE*) was more correlated with $-\log(1/EC_{50})$ than the other descriptors, it is the most important descriptor the regression equations. Besides the total energy (*TE*) descriptor, entropy (S^{o}) is another descriptor that cannot be neglected for constructing the QSAR models.

In series **4**, phenylpropenamides of vinyl bromides compounds, the QSAR equations possessed relative high correlation coefficient with R^2=0.80692, better 31.34498 *F*-statistics, and least number of variables. Some values of EC_{50} of chloro substituted propenamides compounds were greater than 100 μM, which has been been used to calculate -log ($1/EC_{50}$) and participated the linear regression, leading to the R^2 value of series **5** (0.68535) was lower than that of series **4** (0.80692), but it still met the statistical requirements.

The model analysis suggested that the anti-HBV activities of this kind of compounds were mainly affected by molecular total energy (*TE*) and entropy (S^o). The high values of energy was likely to indicate a tendency of the molecule to donate electrons to appropriate acceptors and lower value of energy implies high stability for the molecule in the sense of its lower sensitivity in the biochemical processes [18, 30]. The –log($1/EC_{50}$) was directly proportional to the entropy (S^o) due to the degree of disorder caused by S^o expression and the larger the degree of disorder the lower activities [31].

The correlations between experimental and calculated activities values presented in Fig. 4 indicated that the selected parameters can predict the anti-HBV activities of the set phenylpropenamide molecules with greater predictability. Thus, the new phenylpropenamide molecules with high total energy (*TE*) and low entropy (S^o) may increase the anti-HBV activities.

3.3 3D-QSAR

In the study, the data-based fitting procedure was finally adopted through careful comparison and each analog was superimposed to the template based on the common substructure of propenamide moiety. The aligned molecules were illustrated in Fig. 5 and the statistical parameters were listed in Table 6.

The better predictions are obtained by the 3D-QSAR/CoMFA for anti-HBV activities for phenylpropenamide molecules from Table 6.. The model has a high R^2 (0.980 and 0.986 for series **4** and **5** respectively see in Fig 6) with a low standard deviation(SE, 0.097 and 0.117, respectively) and a high Fischer ratio (*F*, 116.544 and 164.602, respectively); while a QSAR model is generally acceptable if R^2 is approximately 0.9 or higher [33]. Specially, the cross-validation related coefficient q^2 is 0.696 and 0.564 respectively (>0.5) [34], suggesting a good prediction ability of this model [34].

The plots of the predicted versus actual –log($1/EC_{50}$) for the QSAR/CoMFA models were shown in Fig. 6. It could be noted that the data points were uniformly distributed along the regression line. Additionally, all the prediction errors in Table 6 were smaller than 0.5, suggesting the satisfactorily predictive capability, high reliability and accuracy of the models.

To view the field effect on the target property, CoMFA contour maps were generated and shown in Fig. 7. For steric fields, the green was bulky group favorable and yellow was bulky group unfavorable. Similarly, the blue was electropositive charge favorable and red was electronegative charge unfavorable.

For the compounds **4**, the steric field of vinyl bromides of phenylpropenamide molecules with green contours (64.04%) referred to sterically favored regions for anti-HBV activities and yellow contours (35.96%) highlighted the sterically unfavorable regions. The electrostatic field with blue contours (65.32%) represented electropositively preferrable regions to activities and red contours (34.68%) indicated regions where more electronegative substituents are favored. For the compounds **5**, the steric field of vinyl chlorides of phenylpropenamide molecules had green contours (39.22%) refer to sterically favored regions for anti-HBV activities and yellow contours

(60.78%) highlight the sterically unfavorable regions. The electrostatic field had blue contours (29.83%) represent electropositively preferred regions to activities and red contours (70.17%) indicate regions where more electronegative substituents were favored.

For the vinyl bromides series **4a-4r**, the steric field is the dominating factor for the anti-HBV activities and the electrostatic field gave the least contribution. On the contrary, the electrostatic field is the dominating factor for the vinyl chlorides series **5a-5r** for the anti-HBV activities and the steric field effect is the secondary important.

3.4 Comparison between the 2D-QSAR and 3D-QSAR models

The comparison was conducted from two viewpoints of anti-HBV activities mechanism and prediction ability. 2D-QSAR model suggests that both the molecular total energy (*TE*) and entropy (S^{o}) can affect the activities. Judging from 3D-QSAR model, the anti-HBV activities are mainly affected by the steric and electrostatic properties of substituents. Thus, complementary results can be obtained with 2D-QSAR and CoMFA models, which can provide theoretical guide to the application of QSAR in the environmental chemical field.

4. Conclusions

In summary, a series of phenylpropenamide derivatives containing different aromatic ring substituents were synthesized, characterized and assessed for their anti-HBV activities. The quantum chemical parameters of phenylpropenamide derivatives were calculated at the B3LYP/6-311G** level, based on which the 2D-QSAR model of $-\log(1/EC_{50})$ was proposed. The QSAR equations developed with the two parameters total energy (*TE*) and entropy (S^{o}) provided regression models to predict the activity of the set of phenylpropenamide molecules against DNA replication of HBV. The QSAR equation have better stability ability from the values of R^2 (0.80692 and 0.68535), *F*-value (31.34498 and 16.33582) and P (P<0.00010 and P<0.00017) for vinyl bromides and vinyl chlorides respectively. In the mean time, the 3D-QSAR model was proposed by using CoMFA based on the molecular simulation, which also exhibited good stability and prediction ability. The optimum models were all statistically significant with cross-validated coefficients (q^2=0.696 and 0.564) >0.5 and conventional coefficients (R^2=0.980 and 0.986) >0.9, indicating they were reliable enough for activity prediction and providing some insights into the critical structural factors which can affect the bioactivity of phenylpropenamide derivatives. The 3D equipotential map illustrated the effect of different substituent on their anti-HBV activities. The 2D or 3D QSAR models can be utilized to predict the anti-HBV activities of the phenylpropenamide molecules.

Acknowledgements

This work was supported by the NSFC (NO. B020601), Key Laboratory Fund of Sichuan Province(SZJJ2014-081), and the Ministry of Education Innovation Project (No. XZD0912-09)

The authors thank the assistant of Dr. Yang of West china school of pharmacy, Sichuan University for the work of biological assay and thank the students of Prof. Li of College of Chemical engineering, Sichuan University for the work of computational calculations of SYBYL.

Reference

[1] M.F. Sorrell, E.A. Belongia, J. Costa, I.F.Gareen, J.L. Grem, J.M. Inadomi, E.R. Kern, J.A.

McHugh, G.M. Petersen, M.F. Rein, D.B. Strader, H.T. Trotter, Hepatology. 49 (2009) S4-S12.

[2] J.L. Dienstag, N. Engl. J. of Med. 359 (2008) 1486-1500.

[3] M.L. Cui, H.Y. Zhou, J. Liu, W.F. Xu, J. Int. Pharm Res(in chinese). 39 (2012) 280–285.

[4] R.B. Perni, S.C. Conway, S.K. Ladner, K. Zaifert, M.J. Otto, R.W. King, Bioorg. Med. Chem. Lett. 10 (2000) 2687–2690.

[5] G. Fattovich, L. Brollo, A. Alberti, P. Pontisso, G. Giustina, G. Realdi, Hepatology 8 (1988) 1651-1654.

[6] P.Y. Wang, D. Naduthambi, R.T. Mosley, C.R. Niu, P.A. Furman, M.J. Otto, M.J. Sofia, Bioorg. Med. Chem. Lett. 21 (2011) 4642-4647.

[7] Y.Y. Lui, H.L. Chan, Expert Rev. Anti Infect. Ther. 7 (2009) 259-268.

[8] P.N. Cheng, T.T. Chang, Expert Rev. Anti Infect. Ther. 6 (2008) 569-579.

[9] T.A. Shamliyan, R. MacDonald, A. Shaukat, B.C. Taylor, J.M. Yuan, J.R. Johnson, J. Tacklind, I. Rutks, R.L.Kane, T. J. Wilt, Ann. Intern. Med. 150 (2009) 111-124.

[10] W.K Robert, K.L. Stephanie, J.M. Thomas, K. Zatie, B.P. Robert, C.C. Sameul, J.O. Michael, Antimicrobial Agents and Chemotherapy. 42 (1998) 3179-3186.

[11] E.D. William, E.Ros, C. Danni, S. Tim, F. Phil, P. George, L. Stephen, Antimicrobial Agents and Chemotherapy. 46 (2002) 3057-3060.

[12] B. Gaëtan, P. Christian, P. Gerhard, N. Johan, Z. Fabien, Antiviral Research 92 (2011) 271–276.

[13] J.J. Feld, D. Colledge, V. Sozzi, R. Edwards, M. Littlejohn a, S.A. Locarnini, Antiviral Research 76 (2007) 168-177

[14] S.P. Katen, S.R. Chirapu, M.G. Finn, A. Alotnick, Acs.Chem. Biol. 5 (2010) 1125-1136.

[15] R. Hilal, S.A.K. Elroby, Molecular Simulation. 37 (2011) 62-71.

[16] N. Barua, P. Sarmah, I. Hussain, R.C. Deka, A.K. Buragohain, Chem. Biol. Drug. Des, 79 (2012) 553-559.

[17] J. Cao, L.J. Zhao, S.B. Jin, R.G. Zhong, Int. J. of Quan. Chem. 112 (2012) 747-758.

[18] Z.G. Ge, P. Sun, H. Liu, J. Tan, H.X. Liu, Chin. J. Struct. Chem. 30 (2011) 630-637.

[19] S.F. Wu, W. Qi, R.X. Su, T.H. Li, D. Lu, Z.M. He, Eur. J. of Med. Chem. 84 (2014) 100-106.

[20] C.G. Gu, X.H. Ju, X. Jiang, K. Yu, S. Yang, C. Sun, Ecotoxicology and Environmental Safety. 73 (2010) 1470–1479

[21] S.K. Ladner, M.J. Otto, C.S. Barker, K.Zaifert; G.H.Wang, J.T.Guo, C. Seeger, R.W.King, Antimicrob Agents Chemother. 41 (1997) 1715-1720.

[22] R.W. King, S.K. Ladner, T.J. Miller, K. Zaifert, R.B. Perni, S.C. Conway, M.J. Otto, Antimicrob Agents Chemother. 42(1998) 3179-3186.

[23] T.M.C. Tan , Y. Chen, K.H. Kong , J. Bai , Y. Li , S.G. Lim, T.H. Ang, Y. Lam, Antiviral Research. 71 (2006) 7-14.

[24] M.J. Frisch, G.W. Trucks, H.B. Schlegel, G.E. Scuseria, M.A. Robb, J.R. Cheeseman, G. Scalmani, V. Barone, B. Mennucci, G.A. Petersson, H. Nakatsuji, M. Caricato, X. Li, H.P. Hratchian, A.F. Izmaylov, J. Bloino, G. Zheng, J.L. Sonnenberg, M. Hada, M. Ehara, K. Toyota, R. Fukuda, J. Hasegawa, M. Ishida, T. Nakajima, Y. Honda, O. Kitao, H. Nakai, T. Vreven, J.A. Montgomery, Jr., J.E. Peralta, F. Ogliaro, M. Bearpark, J.J. Heyd, E. Brothers, K.N. Kudin, V.N. Staroverov, R. Kobayashi, J. Normand, K. Raghavachari, A. Rendell, J.C. Burant, S.S. Iyengar, J. Tomasi, M. Cossi, N. Rega, J.M. Millam, M. Klene, J.E. Knox, J.B. Cross, V. Bakken, C. Adamo, J. Jaramillo, R. Gomperts, R.E. Stratmann, O. Yazyev, A.J. Austin, R. Cammi, C.

Pomelli, J.W. Ochterski, R.L. Martin, K. Morokuma, V.G. Zakrzewski, G.A. Voth, P. Salvador, J.J. Dannenberg, S. Dapprich, A.D. Daniels, Ö. Farkas, J.B. Foresman, J.V. Ortiz, J. Cioslowski, D.J. Fox, Gaussian, Inc., Wallingford CT, 2009.

[25] M. Clark, R.D. Cramer □, N.V. Opdenbosch, J. Comput. Chem. 10 (1989) 982-1012.

[26] J. Caballero, M. Saavedra, M. Fernández, F.D. González-Nilo, J. Agric. Food Chem. 55 (2007) 8101-8104.

[27] B.L. Bush, R.B. Nachbar, J. Comput Aided Mol. Des. 7 (1993) 587-619.

[28] R.G. Parr and Z. Zhou, Acc. Chem. Res. 26 (1993) 256-258.

[29] R.G. Pearson, Acc. Chem. Res.26 (1993) 250-255.

[30] S. Tahlan, P. Kumar, B. Narasimhan, Drug Res(Stuttg). 64 (2014) 98-103.

[31] C.J. Feng, W.H. Yang, Chin. J. of Struct. Chem. 33 (2014) 830-834.

[32] J.B. Bhonsle, D. Venugopal, D.P. Huddler, A.J. Magill, R.P. Hicks, J. Med. Chem. 50 (2007) 6545-6553.

[33] A.M. Potshangbam, K. Tanneeru, B.M. Reddy, L. Guruprasad, Bioorg.& Med. Chem. Lett. 21 (2011) 7219-7223.

[34] P.P. Roy, J.T. Leonard, K. Roy, Chemom. Intell. Lab. Syst. 90 (2008) 31-42.

Table 1 The anti-HBV activities of compound **4a-4r** and **5a-5r**

Comp.	EC_{50}	$-\log(1/EC_{50})$	Comp.	EC_{50}	$-\log(1/EC_{50})$
4a	1.3	0.113943352	**5a**	1.2	0.079181246
4b	1.1	0.041392685	**5b**	1.7	0.230448921
4c	6.0	0.778151250	**5c**	34.0	1.531478917
4d	10.0	1.000000000	**5d**	51.0	1.707570176
4e	0.9	-0.050609993	**5e**	1.0	-0.004364805
4f	2.8	0.447158031	**5f**	1.1	0.041392685
4g	2.1	0.322219295	**5g**	21.0	1.322219295
4h	8.0	0.903089987	**5h**	25.0	1.397940009
4i	25.0	1.397940009	**5i**	>100.0 [a]	2.000000000
4j	35.0	1.544068044	**5j**	>100.0 [a]	2.000000000
4k	65.0	1.812913357	**5k**	>100.0 [a]	2.000000000
4l	1.5	0.176091259	**5l**	1.8	0.255272505
4m	1.8	0.255272505	**5m**	2.2	0.342422681
4n	8.0	0.903089987	**5n**	39.0	1.591064607
4o	1.0	0.000000000	**5o**	0.9	-0.026872146
4p	7.0	0.845098040	**5p**	30.0	1.477121255
4q	5.0	0.698970004	**5q**	29.0	1.462397998
4r	0.9	-0.045757491	**4r**	0.8	-0.096910013

Table 2 The optimized geometrical parameters of phenylpropenamide derivatives **4a-4r**、**5a-5r**

Comp	Bond length Å					∑Q		
	C=C	C-X (X=Br、Cl)	C-NH	NH-C=O	N-C=O	Ar	Ph	Cy
4a	1.34535	1.95292	1.39645	1.21977	1.22336	-0.896151	-0.919316	-1.775496
4b	1.34332	1.94588	1.39247	1.21853	1.21883	0.348353	-0.844939	-1.688875

4c	1.34201	1.93826	1.39326	1.21925	1.22050	-1.251704	-0.837988	-1.686215
4d	1.34596	1.95194	1.39485	1.21934	1.22326	-1.124014	-0.969986	-1.784969
4e	1.34205	1.96086	1.39710	1.21963	1.22297	-0.461240	-0.825417	-1.749826
4f	1.34530	1.95478	1.39694	1.21988	1.22348	-0.348184	-0.980299	-1.767813
4g	1.34146	1.95776	1.39704	1.22015	1.22103	-1.505460	-0.837188	-1.711406
4h	1.34526	1.95799	1.39733	1.22007	1.22358	-0.627813	-0.959433	-1.760267
4i	1.34221	1.95142	1.39555	1.21947	1.21938	-0.144929	-0.846823	-1.803706
4j	1.34597	1.95021	1.39460	1.21921	1.22293	-0.561815	-0.908448	-1.742217
4k	1.34613	1.95156	1.39462	1.21931	1.22331	-0.555132	-0.959009	-1.777852
4l	1.34218	1.95228	1.39462	1.21930	1.21945	-1.316687	-0.841457	-1.827855
4m	1.34546	1.95320	1.39552	1.21952	1.22329	-0.562458	-0.911908	-1.787560
4n	1.34219	1.95143	1.39515	1.21928	1.21927	-1.062723	-0.827646	-1.782235
4o	1.34633	1.95198	1.39455	1.21929	1.22237	-0.876423	-0.925590	-1.842558
4p	1.34744	1.95151	1.39290	1.21923	1.22302	-1.707655	-0.896693	-1.838197
4q	1.34315	1.95644	1.39495	1.21912	1.22220	-1.030686	-0.833105	-1.769277
4r	1.34807	1.95201	1.39120	1.21876	1.22306	-0.750784	-0.878430	-1.822423
5a	1.34664	1.78686	1.39763	1.21986	1.22395	-1.139492	-0.986517	-1.768942
5b	1.34312	1.78174	1.39419	1.21883	1.21923	-0.014724	-0.932297	-1.748096
5c	1.34186	1.77456	1.39482	1.21960	1.22093	-1.922403	-0.935734	-1.693947
5d	1.34712	1.78663	1.39588	1.21951	1.22380	-1.340251	-1.016954	-1.773090
5e	1.34225	1.79327	1.39846	1.21980	1.22337	-1.096918	-0.916345	-1.752179
5f	1.34655	1.78866	1.39797	1.22006	1.22386	-0.342715	-1.008493	-1.760951
5g	1.34181	1.78996	1.39876	1.22057	1.22166	-1.746778	-0.908333	-1.673087
5h	1.34644	1.79108	1.39843	1.22026	1.22398	-0.978393	-0.992218	-1.755063
5i	1.34255	1.78535	1.39659	1.21961	1.21978	-1.109041	-0.913557	-1.793008
5j	1.34706	1.78488	1.39575	1.21934	1.22370	-0.906464	-0.994730	-1.740841
5k	1.34720	1.78642	1.39559	1.21944	1.22379	-0.765886	-1.013198	-1.765260
5l	1.34228	1.78649	1.39602	1.21947	1.21980	-1.618792	-0.928978	-1.822561
5m	1.34664	1.78749	1.39661	1.21969	1.22381	-0.799893	-0.988045	-1.780463
5n	1.34223	1.78548	1.39679	1.21968	1.21993	-1.759844	-0.938263	-1.788900
5o	1.34757	1.78640	1.39565	1.21936	1.22293	-1.002424	-0.931401	-1.837309
5p	1.34840	1.78615	1.39402	1.21933	1.22350	-1.797908	-0.849097	-1.834680
5q	1.34315	1.78960	1.39654	1.21943	1.22288	-1.484111	-0.926502	-1.788628
5r	1.34883	1.78393	1.39288	1.21912	1.22348	-0.807766	-0.902821	-1.835985

Table 3 The calculation energy value of phenylpropenamide derivatives **4a-4r**、**5a-5r**

Comp.	E_{HOMO} Hartree	E_{LUMO}. Hartree	E_{gap} Hartree	qH^+	α	HF Hartree
4a	-0.062979	-0.226032	0.163053	0.345575	2.5265	-3647.2554986
4b	-0.069673	-0.201043	0.131370	0.352138	6.3080	-3739.5159911
4c	-0.073280	-0.169556	0.096276	0.359610	6.3704	-3851.8084411
4d	-0.068033	-0.230700	0.162667	0.344048	3.4803	-4106.8800729
4e	-0.062275	-0.220858	0.158583	0.345015	2.4387	-3686.5788853
4f	-0.060994	-0.222445	0.161451	0.346774	2.6379	-3686.581249

4g	-0.059536	-0.217935	0.158399	0.351103	1.3644	-3761.805973
4h	-0.063359	-0.225973	0.162614	0.347432	3.9468	-3761.8106142
4i	-0.065055	-0.167983	0.102928	0.345404	3.6920	-6220.7919548
4j	-0.068193	-0.231952	0.163759	0.347991	4.1895	-6220.7988359
4k	-0.071433	-0.231880	0.160447	0.343150	3.4589	-6220.7997101
4l	-0.063786	-0.235357	0.171571	0.350402	3.7022	-3746.5204362
4m	-0.068227	-0.231662	0.163435	0.345640	3.3396	-3746.5259104
4n	-0.064763	-0.199450	0.134687	0.341835	3.7668	-4106.8729964
4o	-0.069899	-0.233532	0.163633	0.350553	4.5745	-3663.2968606
4p	-0.152916	-0.217488	0.064572	0.346016	4.3084	-3816.9741999
4q	-0.077541	-0.218415	0.140874	0.346093	1.2262	-3816.9693588
4r	-0.110853	-0.225450	0.114597	0.338813	2.1350	-3645.0398728
5a	-0.062408	-0.226124	0.163716	0.343903	2.5699	-1533.3355143
5b	-0.068916	-0.200746	0.131830	0.345178	6.2437	-1625.5956197
5c	-0.072831	-0.169381	0.096550	0.356569	6.2551	-1737.8883378
5d	-0.067300	-0.230864	0.163564	0.342664	3.4917	-1992.9601462
5e	-0.061833	-0.220747	0.158914	0.343341	2.4741	-1572.6584057
5f	-0.060514	-0.222493	0.161979	0.343891	2.7166	-1572.6612966
5g	-0.059020	-0.218261	0.159241	0.349448	1.3783	-1647.8855821
5h	-0.062746	-0.225889	0.163143	0.347069	4.0219	-1647.8905643
5i	-0.064564	-0.167614	0.103050	0.344315	3.6592	-4106.8716217
5j	-0.067453	-0.232149	0.164696	0.345872	4.1420	-4106.8789012
5k	-0.067613	-0.230629	0.163016	0.342690	3.4627	-4106.8797531
5l	-0.063872	-0.226796	0.162924	0.351051	3.6575	-1632.5999366
5m	-0.065269	-0.229764	0.164495	0.343537	3.3790	-1632.6059672
5n	-0.064172	-0.199148	0.134976	0.349224	3.6212	-1992.9526691
5o	-0.068952	-0.233662	0.164710	0.340669	4.5732	-1549.3768395
5p	-0.153193	-0.217783	0.064590	0.353758	4.2806	-1703.0541392
5q	-0.077215	-0.218625	0.141410	0.339723	1.1298	-1703.0489175
5r	-0.109331	-0.225701	0.116370	0.341666	2.1974	-1531.119129

Table 4 The calculation thermodynamic parameters of phenylpropenamide derivatives **4a-4r** and **5a-5r**

Comp.	TE Hartree	ZPE Hartree	H^o kJ/mol	G^o kJ/mol	E_{th} KCal/Mol	CV^o Cal/Mol-Kel.	S^o Cal/Mol-Kel.
4a	-3646.851578	-3646.875102	-9574806.34	-9575019.262	253.464	89.559	170.684
4b	-3739.111883	-3739.137333	-9817035.77	-9817261.198	253.582	95.662	180.710
4c	-3851.399743	-3851.425863	-10111847.55	-10112076.16	256.462	98.177	183.267
4d	-4106.484573	-4106.509345	-10781572.77	-10781794.36	248.180	93.421	177.634
4e	-3686.145737	-3686.170868	-9677973.154	-9678193.559	271.805	95.485	176.684
4f	-3686.148181	-3686.173644	-9677979.571	-9678206.112	271.754	95.648	181.604
4g	-3761.367147	-3761.393412	-9875466.963	-9875696.569	275.368	98.839	184.058
4h	-3761.371621	-3761.397774	-9875478.712	-9875707.267	275.472	98.781	183.217
4i	-6220.397092	-6220.422234	-16331650.08	-16331875.56	247.780	93.975	180.748

4j	-6220.403719	-6220.428801	-16331667.49	-16331893.48	247.940	93.885	181.161
4k	-6220.404528	-6220.429537	-16331669.61	-16331893.87	247.981	93.829	179.773
4l	-3746.123963	-3746.148383	-9835445.984	-9835664.924	248.791	92.483	175.508
4m	-3746.129469	-3746.153873	-9835460.442	-9835679.257	248.771	92.572	175.408
4n	-4106.477746	-4106.502637	-10781554.84	-10781778.01	248.023	93.500	178.899
4o	-3662.904804	-3662.928227	-9616954.084	-9617166.957	246.019	88.592	170.644
4p	-3816.533050	-3816.558987	-10020305.04	-10020531.34	276.826	100.279	181.409
4q	-3816.528049	-3816.554110	-10020291.91	-10020519.25	276.926	100.331	182.237
4r	-3644.667102	-3644.689886	-9569070.998	-9569281.229	233.917	85.612	168.529
5a	-1532.931196	-1532.954411	-4024708.377	-4024917.723	253.713	89.104	167.818
5b	-1625.191168	-1625.216357	-4266936.933	-4267159.901	253.797	95.271	178.737
5c	-1737.479300	-1737.505198	-4561749.421	-4561977.036	256.675	97.793	182.461
5d	-1992.564101	-1992.588504	-5231474.57	-5231691.74	248.522	92.866	174.093
5e	-1572.224968	-1572.249918	-4127874.18	-4128093.08	271.986	95.141	175.479
5f	-1572.227813	-1572.252953	-4127881.64	-4128104.06	272.015	95.179	178.299
5g	-1647.446335	-1647.472304	-4325367.87	-4325594.36	275.632	98.399	181.556
5h	-1647.451182	-1647.477033	-4325380.60	-4325605.57	275.717	98.331	180.343
5i	-4106.476273	-4106.501089	-10781550.97	-10781772.93	248.085	93.467	177.924
5j	-4106.483400	-4106.508149	-10781569.69	-10781791.97	248.181	93.415	178.188
5k	-4106.484031	-4106.508699	-10781571.34	-10781791.97	248.319	93.288	176.859
5l	-1632.203176	-1632.227378	-4285346.96	-4285563.71	248.971	92.122	173.754
5m	-1632.209013	-1632.233064	-4285362.28	-4285576.91	249.093	92.041	172.048
5n	-1992.556989	-1992.581561	-5231455.90	-5231675.18	248.293	93.055	175.788
5o	-1548.984370	-1549.007465	-4066855.98	-4067064.78	246.279	88.133	167.377
5p	-1702.612608	-1702.638318	-4470206.92	-4470431.62	277.065	99.875	180.126
5q	-1702.607236	-1702.633038	-4470192.82	-4470418.04	277.159	99.933	180.539
5r	-1530.745978	-1530.768458	-4018971.08	-4019177.61	234.156	85.166	165.557

Table 5 Evaluation and preliminary screening of all the 21 descriptors.

Descriptors	$-\log(1/EC_{50\ \mathbf{4a\text{-}4r}})=a+bX$				$-\log(1/EC_{50\ \mathbf{5a\text{-}5r}})=a+bX$			
	a	b	*R*	*P*	a	b	*R*	*P*
$Å_{C=C}$	1.34426	$2.898378*10^{-4}$	-0.07900	0.75535	1.34546	$-3.80595*10^{-4}$	-0.12184	0.63007
$Å_{C-X}$	1.95331	-0.00155	0.18125	0.47168	1.78713	$-7.6951*10^{-4}$	-0.15821	0.53065
$Å_{C-NH}$	1.39488	$1.20929*10^{-4}$	0.04065	0.87276	1.39626	$-5.13255*10^{-6}$	-0.00258	0.99189
$Å_{NH-C=O}$	1.21938	$3.08097*10^{-5}$	0.04325	0.86469	1.21957	$4.14741*10^{-5}$	0.08373	0.74117
$Å_{N-C=O}$	1.22187	$1.44182*10^{-4}$	0.04832	0.84901	1.22264	$-1.82031*10^{-4}$	-0.08640	0.7332
∑Q of Ar	-0.8735	-0.02518	-0.26526	0.28742	-0.89937	-0.25701	-0.40752	0.09323
∑Q of Ph	-0.80498	0.00485	0.00552	0.98265	-0.94342	-0.00589	-0.10359	0.68251
∑Q of Cy	-1.77528	0.00326	0.04051	0.87319	-1.78788	0.01555	0.28459	0.25237
E_{HOMO}	-0.07385	$-3.10108*10^{-4}$	-0.00782	0.97542	-0.04809	-0.07189	-0.00134	0.8497
E_{LUMO}	-0.22149	0.00709	0.20088	0.42414	-0.22398	0.00782	0.32285	0.1913
E_{gap}	0.14764	-0.0074	0.14114	0.57642	0.15209	-0.00916	-0.25187	0.31334
qH^+	0.34771	$-9.96542*10^{-4}$	-0.12461	0.62227	0.34433	0.00154	0.27741	0.26507
α	3.30838	0.35121	0.14401	0.56861	3.35509	0.16549	0.09901	0.69588

HF	-3340.19581	-1374.54821	-0.83503	<0.0001	-1343.38162	-764.07923	-0.66501	0.00257
TE	-3339.78487	-1374.55001	-0.83502	<0.0001	-1342.97385	-764.07666	-0.66501	0.00260
ZPE	-3339.80945	-1374.55068	-0.83502	<0.0001	-1342.99793	-764.07732	-0.66507	0.00260
H^{e}	$-8.7686*10^{-6}$	$-3.60888*10^{-6}$	-0.83502	<0.0001	$-3.52598*10^{-6}$	$-2.00608*10^{-6}$	-0.66500	0.0026
G^{e}	$-8.76882*10^{-6}$	$-3.60889*10^{-6}$	-0.83502	<0.0001	$-3.52619*10^{-6}$	$-2.00609*10^{-6}$	-0.66500	0.0026
E_{th}	257.86961	-1.12953	-0.04773	0.85083	255.87533	1.61323	0.09776	0.69957
CV^{e}	93.15347	2.14099	0.30715	0.21504	91.74092	2.38453	0.48783	0.04000
S^{e}	175.76684	4.33901	0.53175	0.02313	172.33638	3.75183	0.61512	0.00659

Table 6 The statistical parameters for the best 3D-QSAR CoMFA models

Series	Methods	Statistical results				Filed contribution	
		R^2	F	SE	q^2	Steric	Electrostatic
4a~4r	CoMFA	0.980	116.544	0.097	0.696	0.829	0.171
5a~4r		0.986	164.602	0.117	0.564	0.454	0.546

q^2 =The leave-one-out (LOO) cross-validation coefficient; SE=Standard error of estimate. R^2 =The predictive correlation coefficient; F=test value.

q^2 and R^2 are calculated according to the formula of literature [32]:

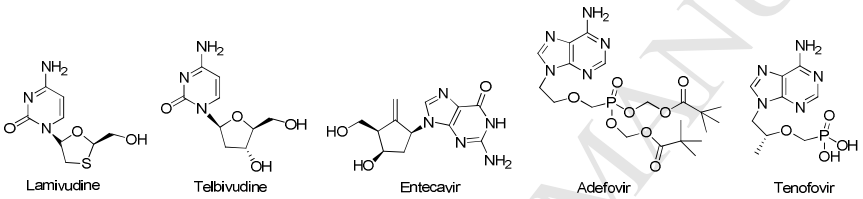

Fig. 1 Agents for the treatment of hepatitis B infection

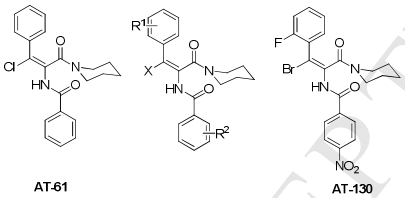

Fig. 2 Structure of phenylpropenamide derivatives

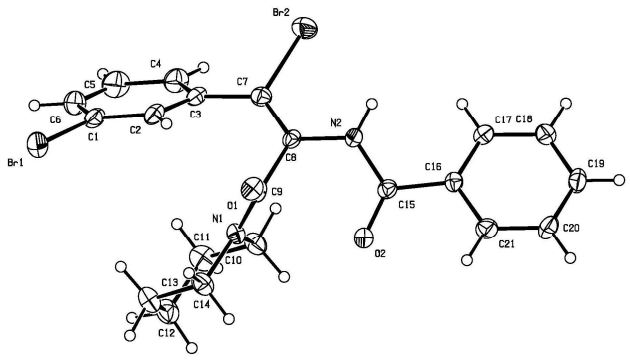

Fig 3: Crystal structure of compound **4j**

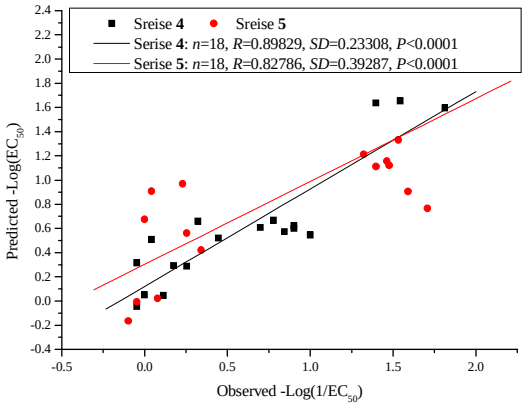

Fig. 4 The Relationships between the -log(1/EC_{50}) values from experiment and prediction based on QSAR equations.

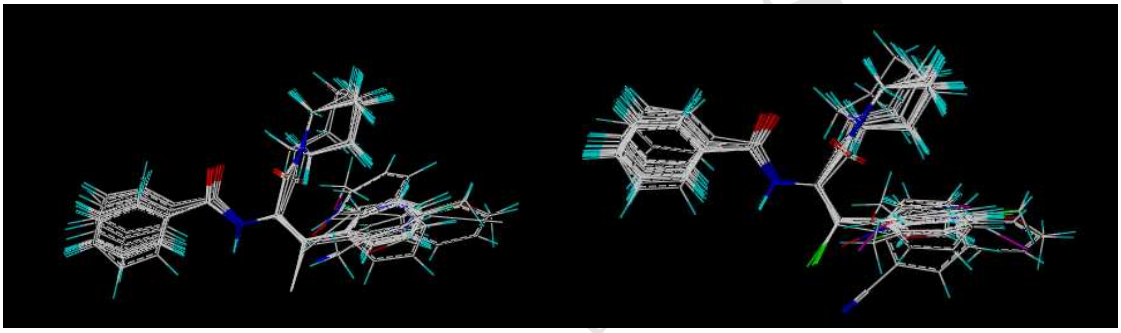

a **b**

Fig. 5 3D-views of all aligned phenylpropenamide molecules(a for series **4** and b for series **5**) congeners by RMSD-based fitting

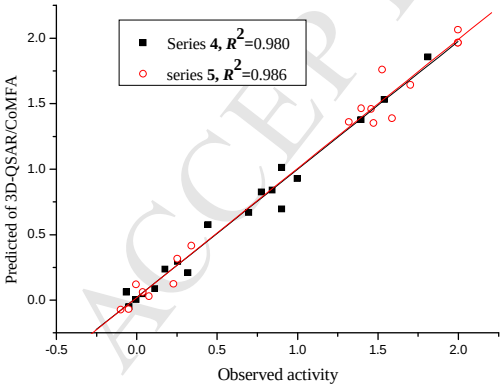

Fig. 6 Plots of experimental activities versus the corresponding predicted activities by QSAR/CoMFA models.

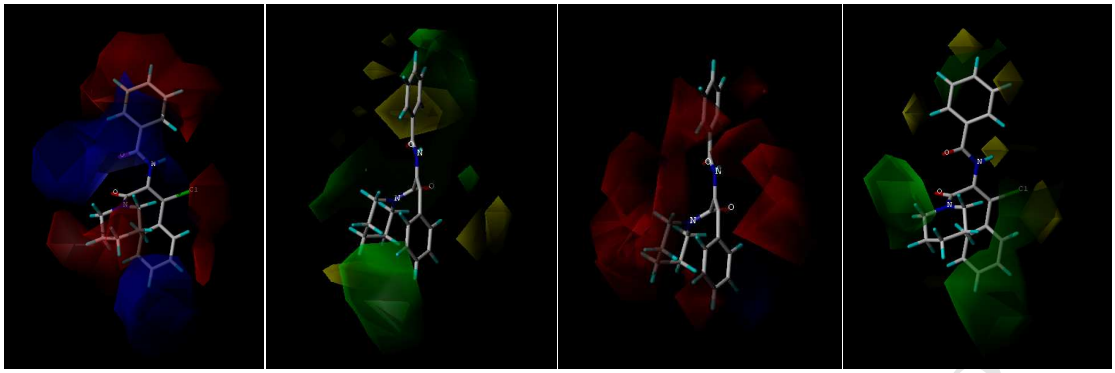

a **b** **c** **d**

Fig. 7. Stereoview of CoMFA electrostatic filed (a) and steric filed (b) of vinyl bromides of phenylpropenamide molecules **4** and electrostatic filed (c) and steric filed (d) of vinyl chlorides of phenylpropenamide molecules **5**

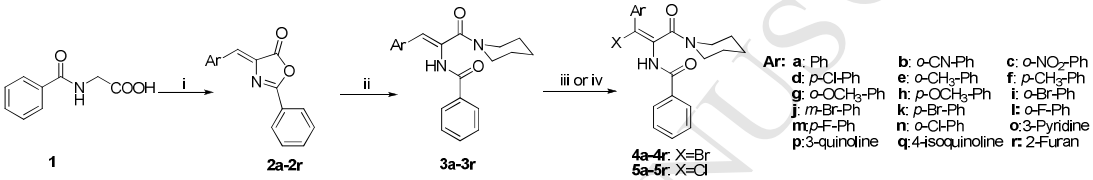

Scheme 1 synthesis of phenylpropenamide derivatives: (i): aromatic aldehydes, AcOK, Ac_2O, reflux; (ii): piperidine, 0□; (iii): Br_2, 0□; (iv): SO_2Cl_2, room temp.

$$-\log\left(\frac{1}{EC_{50\,4a-4r}}\right) = -8.77222 - 4.54623\times 10^{-4}\times TE + 0.04195\times S^{e}$$

Series **4**:n=18, R^2=0.80692, F=31.34498, P<0.0001

$$-\log\left(\frac{1}{EC_{50\,5a-5r}}\right) = -14.57225 - 4.91974\times 10^{-4}\times TE + 0.08248\times S^{e}$$

Series **5**: n=18, R^2=0.68535, F=16.33582, P< 0.00017

Scheme 2: The QSAR equations based on the -log(1/EC_{50}) values

New phenylpropenamide derivatives were synthesized and characterized.

Their 2D-QSAR and model 3D-QSAR were estabilished on DFT and SYBYL respectively.

QSAR model illustrated the effect of substituent on anti-HBV activities.